Improved initial alignment algorithm of SINS on shaking base based on Kalman filter

Ling-Feng Shi (lfshi@mail.xidian.edu.cn)
Xidian University https://orcid.org/0000-0003-2638-9643
Zhi-Yong Hou
Xidian University
Yun-Feng Lv
Xidian University

Research Article

Keywords: Moving Base, Initial Alignment, IAKF, Sequential Filter, Filter Divergence, Smartphone

Posted Date: September 20th, 2022

DOI: https://doi.org/10.21203/rs.3.rs-934909/v1

Improved initial alignment algorithm of SINS on shaking base based on Kalman filter

Ling-Feng Shi (✉) (ORCID: 0000-0003-2638-9643) • Zhi-Yong Hou • Yun-Feng Lv

Institute of Electronic CAD, Xidian University, Xi'an, China

The e-mail address of the corresponding author:

E-mail: lfshi@mail.xidian.edu.cn

Abstract In the initial alignment of shaking base, Kalman filter is easy to diverge, and the alignment result is poor. Many scholars introduce various nonlinear filtering methods to solve this problem, but these filtering methods not only have large amount of calculation, but also are low accuracy. Based on the problem, an improved adaptive Kalman filter (IAKF) algorithm is proposed to complete the initial alignment of the shaking base. The experimental results show that the improved algorithm has high anti-interference and anti-divergence ability. Under the simulation conditions, pitch, roll and heading errors can be stabilized at about 10 degrees. The real measurement with Redmi K30Pro mobile phone shows that the alignment result of the improved algorithm is consistent, and the difference of multiple alignment results is stable within 5 degrees, while the difference of traditional method is more than 20 degrees. It can be applied in smart phone navigation with the strapdown inertial navigation system.

Keywords Moving Base • Initial Alignment • IAKF • Sequential Filter • Filter Divergence • Smartphone

1 Introduction

The strapdown inertial navigation system (SINS) uses the gyroscope and accelerometer data to calculate the attitude, speed and position of the carrier [1]. It can work independently without relying on external information, and it will not radiate any information to the outside world during work [2] [3]. Because of its low cost and portable equipment, it has developed rapidly once it is proposed, and has a very important position in the navigation field.

Before SINS starts to work because the carrier coordinate system is completely unknown to the navigation reference coordinate system, the initial alignment is required [4] [5], that is, SINS needs to be determined before starting work. The spatial orientation of the carrier coordinate system relative to the navigation reference coordinate system (generally the geographic coordinate system with the three-axis pointing to the "North-East Sky") is essentially the process of finding the navigation reference coordinate system. The accuracy of the initial alignment is critical to the performance of the subsequent inertial navigation, and the poor alignment effect will cause the subsequent inertial navigation solution to quickly diverge and lose its meaning. At the same time, the time consumption of alignment is also an important criterion. In the military field, if the alignment time is too long, even if the result is excellent, it is meaningless. Therefore, how to complete the initial alignment quickly and accurately has always been a hot topic.

The initial alignment of SINS can usually be divided into two stages [6]: coarse alignment stage and fine alignment stage. In the coarse alignment stage, the measurement output of the inertial device is usually used to obtain a rough matrix of the initial attitude; in the alignment stage, an algorithm is used to estimate the misalignment angle of the coarse alignment result to further correct the error of the coarse alignment.

At present, there are many methods used in the fine alignment stage. The most commonly used method is the Kalman filter method based on the "prediction + correction" idea [7] [8]. The error equation is established based on the dynamic model to determine the attitude parameters, and related error sources are estimated and compensated in real time. However, Kalman filter is usually only suitable for linear systems and is very sensitive to system parameters and noise parameters. Kalman filter can obtain the optimal state estimation only when the system's result parameters and noise statistics are known accurately. However, in actual SINS applications, due to the continuous changes in the surrounding environment, it is impossible to obtain accurate system result parameters and noise statistical characteristic parameters. Usually, the estimated measurement noise variance matrix parameters may be different from the empirical value. In this case, the accuracy of the Kalman filter will be severely limited, and even cause divergence. Using inaccurate measurement noise parameters for Kalman filter will decrease the accuracy and speed of the results. Based on this, many scholars have proposed different improved filtering methods. In [9], an improved CKF based on Bayesian theory and spherical diameter criterion is used to ensure the stability of the filtering process and further improve the calculation speed of traditional CKF. In [10], an algorithm based on the combination of innovation adaptive estimation and extended Kalman filter is proposed for alignment, but this method requires GPS information to assist in alignment, and the algorithm is complex to implement, the equipment structure is complex, and the use of scenarios is popularized. In [11], the iterative process of measuring noise covariance is re-derived, combined with the variational adaptive algorithm to improve the Kalman filter algorithm, which improves the computational efficiency.

Up to now, many adaptive estimation algorithms [12] have been used to estimate the noise parameters in the Kalman filter process to suppress the divergence of the Kalman filter, such as innovation-based AKF [13], the expectation maximization- based AKF [14] etc. There are also many variants of Kalman filtering and fusion filtering algorithms to suppress divergence, such as Unscented Kalman Filter (UKF) [15], Extended Kalman Filter (EKF) [16], Elimination of Kalman filter [17], genetic filter algorithm, and so on.

The improved adaptive Kalman filter algorithm proposed in the paper uses the update of the noise covariance matrix in the Kalman filter process as the entry point. In the update process, the sequential filtering idea is used for group update, and fault detection and judgment are performed for each update. According to the results of the evaluation, different update methods are selected to improve the stability of the filter, and then the control function is added to the gain matrix calculation of the Kalman filter to accelerate the speed of approximating the true value.

The structure of this paper is as follows. Section 2 describes the establishment of the initial alignment model of SINS and the related work of filtering algorithm derivation. In section 3, the experimental simulation results and discussion are given. Finally, section 4 summarizes the conclusions.

2 Initial Alignment Model Establishment and Filtering Algorithm Derivation

The flow chart of SINS is shown in Fig. 1.

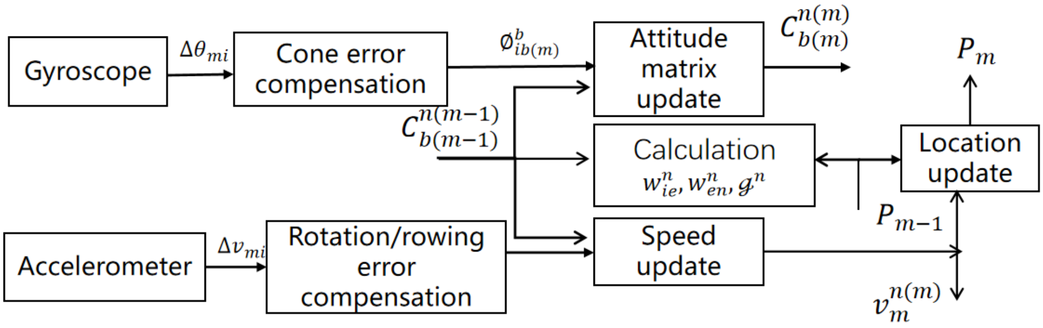

Fig. 1 Flow chart of SINS

The system model in this paper is based on Yan Gongmin's simplified linear SINS error model [18], and the model is described as follows:

$$\begin{cases} \mathbf{X} = \mathbf{F}\mathbf{X}^T + \mathbf{G}\mathbf{W}^b \\ \mathbf{Z} = \mathbf{H}\mathbf{X}^T + \mathbf{V} \end{cases} \tag{1}$$

where,

$$\mathbf{X} = [\phi_E \quad \phi_N \quad \phi_U \quad \delta v_E \quad \delta v_N \quad \delta v_U \quad \varepsilon^b_x \quad \varepsilon^b_y \quad \varepsilon^b_z \quad \nabla^b_x \quad \nabla^b_y \quad \nabla^b_z]$$

$$\mathbf{F} = \begin{bmatrix} -(\boldsymbol{\omega}^n_{ie}\times) & \mathbf{0}_{3\times3} & -\mathbf{C}^n_b & \mathbf{0}_{3\times3} \\ -|(\mathbf{g}^n\times) & \mathbf{0}_{3\times3} & \mathbf{0}_{3\times3} & \mathbf{C}^n_b \\ & \mathbf{0}_{6\times12} & & \end{bmatrix}$$

$$\mathbf{G} = \begin{bmatrix} -\mathbf{C}^n_b & \mathbf{0}_{3\times3} \\ \mathbf{0}_{3\times3} & \mathbf{C}^n_b \\ \mathbf{0}_{6\times6} & \end{bmatrix}$$

$$\mathbf{W}^b = [w^b_{gx} \quad w^b_{gy} \quad w^b_{gz} \quad w^b_{ax} \quad w^b_{ay} \quad w^b_{az}]^T$$

$$\mathbf{H} = [\mathbf{0}_{3\times3} \quad \mathbf{I}_{3\times3} \quad \mathbf{0}_{3\times6}],\ \mathbf{V} = [V_E \quad V_N \quad V_U]^T$$

The above model is the fine alignment model used in this paper for initial alignment under shaking interference, and the subsequent alignment algorithm is based on this model.

2.1 Standard Kalman filter

Assuming a discrete linear system, its state equation and measurement equation are shown in (2):

$$\begin{cases} \mathbf{x}_k = \boldsymbol{\Phi}_{k|k-1}\mathbf{x}_{k-1} + \boldsymbol{\Gamma}_{k-1}\mathbf{w}_{k-1} \\ \mathbf{z}_k = \mathbf{H}_k\mathbf{x}_k + \mathbf{v}_k \end{cases} \tag{2}$$

where $\mathbf{x}_k$ is the state vector, $\mathbf{z}_k$ is the measurement vector, $\boldsymbol{\Phi}_{k|k-1}$ represents the state transition matrix, $\boldsymbol{\Gamma}_k$ is the noise allocation matrix, and $\mathbf{H}_k$ notes Measurement matrix, $\mathbf{w}_k$ represents system noise, $\mathbf{v}_k$ is measurement noise.

And meet the following conditions: $E[\mathbf{w}_k] = 0, E[\mathbf{w}_k\mathbf{w}^T_j] = \delta_{kj}\mathbf{Q}_k, E[\mathbf{v}_k] = 0,\quad E[\mathbf{v}_k\mathbf{v}^T_j] = \delta_{kj}\mathbf{R}_k$, $E[\mathbf{w}_k\mathbf{v}^T_j] = 0$, where δ_{kj} is the Dirac function.

In a discrete linear system, the optimal estimated value of the state vector $\mathbf{x}_k$ is $\hat{\mathbf{x}}_k$, and Kalman filter uses the measurement vector $\mathbf{z}_k$ to pass the following five steps to obtain this optimal estimate:

(1) The one-step prediction calculation process of the state is as follows:

$$\hat{\mathbf{x}}_{k|k-1} = \mathbf{\Phi}_{k|k-1}\hat{\mathbf{x}}_{k-1}$$

(2) Calculate the one-step prediction mean square error matrix:

$$\mathbf{P}_{k|k-1} = \mathbf{\Phi}_{k|k-1}\mathbf{P}_{k-1}\mathbf{\Phi}_{k|k-1}^T + \mathbf{\Gamma}_{k-1}\mathbf{Q}_{k-1}\mathbf{\Gamma}_{k-1}^T$$

(3) Calculate the weighted value of the previous estimated value and the difference between the measured value and the estimated value, also called the filter gain matrix:

$$\mathbf{K}_k = \mathbf{P}_{k|k-1}\mathbf{H}_k^T\left(\mathbf{H}_k\mathbf{P}_{k|k-1}\mathbf{H}_k^T + \mathbf{R}_k\right)^{-1}$$

(4) The optimal state estimation can be calculated by the following equation:

$$\hat{\mathbf{x}}_k = \hat{\mathbf{x}}_{k|k-1} + \mathbf{K}_k(\mathbf{z}_k - \mathbf{H}_k\hat{\mathbf{x}}_{k|k-1})$$

(5) Calculate the state estimation mean square error matrix:

$$\mathbf{P}_k = (\mathbf{I} - \mathbf{K}_k\mathbf{H}_k)\mathbf{P}_{k|k-1}$$

Summarized as follows:

$$\begin{cases} \hat{\mathbf{x}}_{k|k-1} = \mathbf{\Phi}_{k|k-1}\hat{\mathbf{x}}_{k-1} \\ \mathbf{P}_{k|k-1} = \mathbf{\Phi}_{k|k-1}\mathbf{P}_{k-1}\mathbf{\Phi}_{k|k-1}^T + \mathbf{\Gamma}_{k-1}\mathbf{Q}_{k-1}\mathbf{\Gamma}_{k-1}^T \\ \mathbf{K}_k = \mathbf{P}_{k|k-1}\mathbf{H}_k^T(\mathbf{H}_k\mathbf{P}_{k|k-1}\mathbf{H}_k^T + \mathbf{R}_k)^{-1} \\ \hat{\mathbf{x}}_k = \hat{\mathbf{x}}_{k|k-1} + \mathbf{K}_k(\mathbf{z}_k - \mathbf{H}_k\hat{\mathbf{x}}_{k|k-1}) \\ \mathbf{P}_k = (\mathbf{I} - \mathbf{K}_k\mathbf{H}_k)\mathbf{P}_{k|k-1} \end{cases} \tag{3}$$

If the measurement prediction is $\hat{\mathbf{z}}_{k|k-1} = \mathbf{H}_k\hat{\mathbf{x}}_{k|k-1}$, the covariance between the state prediction error and the measurement prediction error is $\mathbf{P}_{xy,k|k-1} = E[(\hat{\mathbf{x}}_{k|k-1} - \mathbf{x}_k)(\hat{\mathbf{z}}_{k|k-1} - \mathbf{z}_k)]^T$. Then there is (4):

$$\begin{aligned} \mathbf{P}_{xy,k|k-1} &= E[(\hat{\mathbf{x}}_{k|k-1} - \mathbf{x}_k)(\mathbf{H}_k\hat{\mathbf{x}}_{k|k-1} - \mathbf{H}_k\mathbf{x}_k - \mathbf{v}_k)^T] \\ &= E[(\hat{\mathbf{x}}_{k|k-1} - \mathbf{x}_k)(\hat{\mathbf{x}}_{k|k-1} - \mathbf{x}_k)^T]\mathbf{H}_k^T = \mathbf{P}_{k|k-1}\mathbf{H}_k^T \end{aligned} \tag{4}$$

Measure the mean square error of the prediction error as $\mathbf{P}_{y,k|k-1} = E[(\hat{\mathbf{z}}_{k|k-1} - \mathbf{z}_k)(\hat{\mathbf{z}}_{k|k-1} - \mathbf{z}_k)^T]$, then

$$\begin{aligned} \mathbf{P}_{y,k|k-1} &= E[(\mathbf{H}_k\hat{\mathbf{x}}_{k|k-1} - \mathbf{H}_k\mathbf{x}_k - \mathbf{v}_k)(\mathbf{H}_k\hat{\mathbf{x}}_{k|k-1} - \mathbf{H}_k\mathbf{x}_k - \mathbf{v}_k)^T] \\ &= \mathbf{H}_k E[(\hat{\mathbf{x}}_{k|k-1} - \mathbf{x}_k)(\hat{\mathbf{x}}_{k|k-1} - \mathbf{x}_k)^T]\mathbf{H}_k^T + E[\mathbf{v}_k\mathbf{v}_k^T] \\ &= \mathbf{H}_k\mathbf{P}_{k|k-1}\mathbf{H}_k^T + \mathbf{R}_k \end{aligned} \tag{5}$$

Substituting (4) and (5) into the above filter gain calculation equation, we can get (6):

$$\mathbf{K}_k = \mathbf{P}_{xy,k|k-1}\mathbf{P}_{y,k|k-1}^{-1} \tag{6}$$

The state estimation mean square error matrix $\mathbf{P}_k$ can be written as (7):

$$\mathbf{P}_k = \mathbf{P}_{k|k-1} - \mathbf{K}_k\mathbf{P}_{y,k-1}\mathbf{K}_k^T \tag{7}$$

In summary, the Kalman filter recurrence equation can also be written as following:

$$
\begin{cases}
\hat{\mathbf{x}}_{k|k-1} = \mathbf{\Phi}_{k|k-1}\hat{\mathbf{x}}_{k-1} \\
\mathbf{P}_{k|k-1} = \mathbf{\Phi}_{k|k-1}\mathbf{P}_{k-1}\mathbf{\Phi}_{k|k-1}^{T} + \mathbf{\Gamma}_{k-1}\mathbf{Q}_{k-1}\mathbf{\Gamma}_{k-1}^{T} \\
\mathbf{P}_{xy,k|k-1} = \mathbf{P}_{k|k-1}\mathbf{H}_{k}^{T}, \mathbf{P}_{\hat{z}_k\hat{z}_k} = \mathbf{H}_{k}\mathbf{P}_{k|k-1}\mathbf{H}_{k}^{T} + \mathbf{R}_{k} \\
\mathbf{K}_{k} = \mathbf{P}_{xy,k|k-1}\mathbf{P}_{y,k|k-1} \\
\hat{\mathbf{z}}_{k} = \mathbf{H}_{k}\hat{\mathbf{x}}_{k|k-1}, \hat{\mathbf{x}}_{k} = \hat{\mathbf{x}}_{k|k-1} + \mathbf{K}_{k}(\mathbf{z}_{k} - \hat{\mathbf{z}}_{k|k-1}) \\
\mathbf{P}_{k} = \mathbf{P}_{k|k-1} - \mathbf{K}_{k}\mathbf{P}_{y,k|k-1}\mathbf{K}_{k}^{T}
\end{cases} \tag{8}
$$

2.2 Combining sequential inertial filtering to improve adaptive Kalman filtering

In Kalman filtering, the equation for measuring the prediction error (that is innovation) is (9):

$$\tilde{\mathbf{Z}}_{k|k-1} = \mathbf{Z}_{k} - \hat{\mathbf{Z}}_{k|k-1} = \mathbf{H}_{k}\mathbf{X}_{k} + \mathbf{V}_{k} - \mathbf{H}_{k}\hat{\mathbf{X}}_{k|k-1} = \mathbf{H}_{k}\hat{\mathbf{X}}_{k|k-1} + \mathbf{V}_{k} \tag{9}$$

When the state is initially selected unbiased, the state one-step prediction error $\tilde{\mathbf{X}}_{k|k-1}$ s unbiased, and then the mean value of measurement noise $\mathbf{V}_k$ is zero. We know that the mean value of innovation $\tilde{\mathbf{Z}}_{k|k-1}$ is also zero. Further considering that $\tilde{\mathbf{X}}_{k|k-1}$ and $\mathbf{V}_k$ are uncorrelated with each other, the variance of both sides of (9) is calculated at the same time. We can get (10):

$$E[\tilde{\mathbf{Z}}_{k|k-1}\tilde{\mathbf{Z}}_{k|k-1}^{T}] = \mathbf{H}_{k}\mathbf{P}_{k|k-1}\mathbf{H}_{k}^{T} + \mathbf{R}_{k} \tag{10}$$

Shift the term to obtain the measurement noise variance matrix Rk in (11):

$$\mathbf{R}_{k} = E[\tilde{\mathbf{Z}}_{k|k-1}\tilde{\mathbf{Z}}_{k|k-1}^{T}] - \mathbf{H}_{k}\mathbf{P}_{k|k-1}\mathbf{H}_{k}^{T} \tag{11}$$

In (11), $E[\tilde{\mathbf{Z}}_{k|k-1}\tilde{\mathbf{Z}}_{k|k-1}^{T}]$ theoretically represents the lumped average of random sequences. In this paper, time average is used instead, and the equal-weighted recursive estimation method of $\mathbf{R}_k$ is constructed in (12):

$$
\begin{aligned}
\hat{\mathbf{R}}_{k} &= \frac{1}{k}\sum_{i=1}^{k}(\tilde{\mathbf{Z}}_{i|i-1}\tilde{\mathbf{Z}}_{i|i-1}^{T} - \mathbf{H}_{i}\mathbf{P}_{i|i-1}\mathbf{H}_{i}^{T}) \\
&= \frac{1}{k}[\sum_{i=1}^{k-1}(\tilde{\mathbf{Z}}_{i|i-1}\tilde{\mathbf{Z}}_{i|i-1}^{T} - \mathbf{H}_{i}\mathbf{P}_{i|i-1}\mathbf{H}_{i}^{T}) + (\tilde{\mathbf{Z}}_{k|k-1}\tilde{\mathbf{Z}}_{k|k-1}^{T} - \mathbf{H}_{k}\mathbf{P}_{k|k-1}\mathbf{H}_{k}^{T})] \\
&= \frac{1}{k}[(k-1)\hat{\mathbf{R}}_{k-1} + (\tilde{\mathbf{Z}}_{k|k-1}\tilde{\mathbf{Z}}_{k|k-1}^{T} - \mathbf{H}_{k}\mathbf{P}_{k|k-1}\mathbf{H}_{k}^{T})] \\
&= (1-\frac{1}{k})\hat{\mathbf{R}}_{k-1} + \frac{1}{k}(\tilde{\mathbf{Z}}_{k|k-1}\tilde{\mathbf{Z}}_{k|k-1}^{T} - \mathbf{H}_{k}\mathbf{P}_{k|k-1}\mathbf{H}_{k}^{T})
\end{aligned} \tag{12}
$$

Among them, the initial value $\hat{\mathbf{R}}_0$ is the variance matrix that matches the reality.

In (12), when $k \to \infty$, there is $1/k \to 0$, that is, the adaptive ability will gradually weaken after a long period of filtering until the adaptive effect is almost lost. In order to always maintain an appropriate size of adaptive ability, this paper combines the adaptive filtering to change the equal weighted equation to the following exponential weighted average (13) and (14):

$$\hat{\mathbf{R}}_{k} = (1-\beta_k)\hat{\mathbf{R}}_{k-1} + \beta_k(\tilde{\mathbf{Z}}_{k|k-1}\tilde{\mathbf{Z}}_{k|k-1}^{T} - \mathbf{H}_{k}\mathbf{P}_{k|k-1}\mathbf{H}_{k}^{T}) \tag{13}$$

$$\beta_k = \frac{\beta_{k-1}}{\beta_{k-1} + b} \tag{14}$$

where, the paper sets the initial value β_0=1, and the attenuation factor b is 0.95. Adjusting the size of the attenuation factor can control the algorithm's adaptive ability to the new measured noise changes. The smaller the value, the stronger the adaptive ability.

Observation (13), if the theoretical modeling value is greater than the measurement noise of the actual system, $\tilde{\mathbf{Z}}_{k|k-1}\tilde{\mathbf{Z}}_{k|k-1}^T$ will be relatively small; if the initial state noise is too large, $\mathbf{H}_k\mathbf{P}_{k|k-1}\mathbf{H}_k^T$ will be relatively large. The above situations have a chance to cause $\tilde{\mathbf{Z}}_{k|k-1}\tilde{\mathbf{Z}}_{k|k-1}^T-\mathbf{H}_k\mathbf{P}_{k|k-1}\mathbf{H}_k^T$ <0, so that it is easy to make $\hat{\mathbf{R}}_k$ loses positive definiteness to cause abnormal filtering. This paper originals from the idea of fault detection and isolation, adopts the sequential filtering method to perform sequential measurement update on the noise matrix $\hat{\mathbf{R}}_k$, and adds a detection mechanism in the update process according to different. The detection results choose different update calculation methods to limit the size of each element of $\hat{\mathbf{R}}_k$ diagonal. The specific implementation is as follows:

Firstly, the measurement equation for sequential update of the *i*-th scalar is (15):

$$\mathbf{Z}_k^{(i)}=\mathbf{H}_k^{(i)}\mathbf{X}_k+\mathbf{V}_k^{(i)} \tag{15}$$

Abbreviation

$$\rho_k^{(i)}=(\mathbf{Z}_{k|k-1}^{(i)})^2-\mathbf{H}_k^{(i)}\mathbf{P}_{k|k-1}^{(i)}(\mathbf{H}_k^{(i)})^T \tag{16}$$

Use $\rho_k^{(i)}$ as the judgment condition. If it is less than the lower limit $\mathbf{R}_{\min}^{(i)}$, use $(1-\beta_k)\hat{\mathbf{R}}_{k-1}^{(i)}+\beta_k\mathbf{R}_{\min}^{(i)}$ to update the measurement noise to ensure $\hat{\mathbf{R}}_k^{(i)}$ is positive; if it is greater than the upper limit $\hat{\mathbf{R}}_{\max}^{(i)}$, it is considered that the filtering is abnormal, the update is abandoned, and the upper limit is directly used as the update result; If in between them, use $(1-\beta_k)\hat{\mathbf{R}}_{k-1}^{(i)}+\beta_k\rho_k^{(i)}$ to update. $\hat{\mathbf{R}}_k^{(i)}$ calculation method in this paper is as follows (17):

$$\hat{\mathbf{R}}_k^{(i)}=\begin{cases}(1-\beta_k)\hat{\mathbf{R}}_{k-1}^{(i)}+\beta_k\mathbf{R}_{\min}^{(i)} & (\rho_k^{(i)}<\mathbf{R}_{\min}^{(i)})\\ \mathbf{R}_{\max}^{(i)} & (\rho_k^{(i)}>\mathbf{R}_{\max}^{(i)})\\ (1-\beta_k)\hat{\mathbf{R}}_{k-1}^{(i)}+\beta_k\rho_k^{(i)} & (\text{other})\end{cases} \tag{17}$$

Through the above processing, the measurement noise $\hat{\mathbf{R}}_k^{(i)}$ can always be limited to the interval [$\mathbf{R}_{\min}^{(i)}$, $\mathbf{R}_{\max}^{(i)}$], which has better adaptive ability and filtering reliability. In the paper, the initial value of $\mathbf{R}_{\min}$ is set to 0.01*$\mathbf{R}_0$, and the initial value of $\mathbf{R}_{\max}$ is set to 100*$\mathbf{R}_0$.

Secondly, in order to add a large number of measurements to the state estimation, the paper combines the fading factor filtering algorithm to improve the process of gain matrix update in the Kalman filtering process. From (10), if the modeling is accurate, the variance matrix of the innovation sequence of the standard Kalman filter can be written as (18):

$$E[\tilde{\mathbf{Z}}_{k|k-1}\tilde{\mathbf{Z}}_{k|k-1}^T]=\mathbf{H}_k(\mathbf{\Phi}_{k|k-1}\mathbf{P}_{k-1}\mathbf{\Phi}_{k|k-1}^T+\mathbf{\Gamma}_{k-1}\mathbf{Q}_{k-1}\mathbf{\Gamma}_{k-1}^T)\mathbf{H}_k^T+\mathbf{R}_k \tag{18}$$

From the real filtered innovation time series, the following variance matrix is estimated (19):

$$\hat{\mathbf{C}}_k=(1-\beta_k)\hat{\mathbf{C}}_{k-1}+\beta_k\tilde{\mathbf{Z}}_{k|k-1}\tilde{\mathbf{Z}}_{k|k-1}^T \tag{19}$$

(18) and (17) should be consistent, therefore

$$\hat{\mathbf{C}}_k\approx\mathbf{H}_k(\mathbf{\Phi}_{k|k-1}\mathbf{P}_{k-1}\mathbf{\Phi}_{k|k-1}^T+\mathbf{\Gamma}_{k-1}\mathbf{Q}_{k-1}\mathbf{\Gamma}_{k-1}^T)\mathbf{H}_k^T+\mathbf{R}_k \tag{20}$$

Shift items available

$$\hat{\mathbf{C}}_k-\mathbf{H}_k\mathbf{\Gamma}_{k-1}\mathbf{Q}_{k-1}\mathbf{\Gamma}_{k|k-1}^T\mathbf{H}_k^T-\mathbf{R}_k\approx\mathbf{H}_k\mathbf{\Phi}_{k|k-1}\mathbf{P}_{k-1}\mathbf{\Phi}_{k|k-1}^T\mathbf{H}_k^T \tag{21}$$

If the system parameters $\mathbf{\Phi}_{k|k-1}$, $\mathbf{\Gamma}^T_{k-1}$, $\mathbf{H}_k$, $\mathbf{Q}_k$ or $\mathbf{R}_k$ is not accurate enough, as the filtering progresses, the accuracy of the state estimation may deteriorate, leading to a mismatch of innovation. Therefore, the calculation method of the state estimation mean square error matrix $\mathbf{P}_{k-1}$ needs to be adjusted. Modify the above (21) as follows (22):

$$\hat{\mathbf{C}}_k - \mathbf{H}_k\mathbf{\Gamma}_{k-1}\mathbf{Q}_{k-1}\mathbf{\Gamma}^T_{k-1}\mathbf{H}^T_k - \mathbf{R}_k = \mathbf{H}_k\mathbf{\Phi}_{k|k-1}(\lambda_k\mathbf{P}_{k-1})\mathbf{\Phi}^T_{k|k-1}\mathbf{H}^T_k \tag{22}$$

Perform matrix trace calculation on both ends of (22) at the same time, considering that the proportional coefficient λ_k should not be less than 1, we can get (23)

$$\lambda_k = \max(1, \frac{\mathrm{tr}(N_k)}{\mathrm{tr}(M_k)}) \tag{23}$$

where,

$$\begin{aligned} N_k &= \hat{\mathbf{C}}_k - \mathbf{H}_k\mathbf{\Gamma}_{k-1}\mathbf{Q}_{k-1}\mathbf{\Gamma}^T_{k-1}\mathbf{H}^T_k - \mathbf{R}_k \\ M_k &= \mathbf{H}_k\mathbf{\Phi}_{k|k-1}\mathbf{P}_{k-1}\mathbf{\Phi}^T_{k|k-1}\mathbf{H}^T_k \end{aligned} \tag{24}$$

Therefore, the state estimation mean square error matrix $\mathbf{P}_{k-1}$ can be calculated as follows (25):

$$\mathbf{P}_{k|k-1} = \mathbf{\Phi}_{k|k-1}(\lambda_k\mathbf{P}_{k-1})\mathbf{\Phi}^T_{k|k-1} + \mathbf{\Gamma}_{k-1}\mathbf{Q}_{k-1}\mathbf{\Gamma}^T_{k-1} \tag{25}$$

It can be seen that when the innovation is mismatched, λ_k >1, (25) will amplify $\mathbf{P}_{k-1}$ so that the filter gain $\mathbf{K}_k$ becomes larger, and a large number of test pairs are added. The correction effect of the state estimation is to track the changes of the measurement more quickly; when there is no innovation mismatch λ_k =1, (25) is the same as before the improvement, and it also has the optimal state estimation.

The IAKF process in this paper is following:

$$\begin{cases} \hat{\mathbf{x}}_{k|k-1} = \mathbf{\Phi}_{k|k-1}\hat{\mathbf{x}}_{k-1} \\ \mathbf{P}_{k|k-1} = \mathbf{\Phi}_{k|k-1}(\lambda_k\mathbf{P}_{k-1})\mathbf{\Phi}^T_{k|k-1} + \mathbf{\Gamma}_{k-1}\mathbf{Q}_{k-1}\mathbf{\Gamma}^T_{k-1} \\ \mathbf{P}_{xy,k|k-1} = \mathbf{P}_{k|k-1}\mathbf{H}^T_k, \mathbf{P}_{\hat{z}_k\hat{z}_k} = \mathbf{H}_k\mathbf{P}_{k|k-1}\mathbf{H}^T_k + \mathbf{R}_k \\ \mathbf{K}_k = \mathbf{P}_{xy,k|k-1}\mathbf{P}_{y,k|k-1} \\ \hat{\mathbf{z}}_k = \mathbf{H}_k\hat{\mathbf{x}}_{k|k-1}, \hat{\mathbf{x}}_k = \hat{\mathbf{x}}_{k|k-1} + \mathbf{K}_k(\mathbf{z}_k - \hat{\mathbf{z}}_{k|k-1}) \\ \mathbf{P}_k = \mathbf{P}_{k|k-1} - \mathbf{K}_k\mathbf{P}_{y,k|k-1}\mathbf{K}^T_k \end{cases} \tag{26}$$

$$\begin{cases} \hat{\mathbf{r}}_k = (1 - 1/k)\hat{\mathbf{r}}_{k-1} + (\mathbf{y}_k - \mathbf{H}_k\hat{\mathbf{x}}_{k|k-1})/k \\ \hat{\mathbf{R}}^{(i)}_k = \begin{cases} (1-\beta_k)\hat{\mathbf{R}}^{(i)}_{k-1} + \beta_k\mathbf{R}^{(i)}_{\min} & (\rho^{(i)}_k < \mathbf{R}^{(i)}_{\min}) \\ \mathbf{R}^{(i)}_{\max} & (\rho^{(i)}_k > \mathbf{R}^{(i)}_{\max}) \\ (1-\beta_k)\hat{\mathbf{R}}^{(i)}_{k-1} + \beta_k\rho^{(i)}_k & (\text{other}) \end{cases} \\ \hat{\mathbf{q}}_{k-1} = (1 - 1/k)\hat{\mathbf{q}}_{k-2} + (\hat{\mathbf{x}}_k - \mathbf{\Phi}_{k|k-1}\hat{\mathbf{x}}_{k-1})/k \\ \hat{\mathbf{Q}}_{k-1} = (1 - 1/k)\hat{\mathbf{Q}}_{k-2} - (\mathbf{K}_k\mathbf{e}_{y,k|k-1}\mathbf{e}^T_{y,k|k-1}\mathbf{K}^T_k \end{cases} \\ \quad + \mathbf{P}_{x,k} - \mathbf{\Phi}_{k|k-1}\mathbf{P}_{x,k-1}\mathbf{\Phi}^T_{k|k-1} \tag{27}$$

3. Experimental Verification

3.1 Matlab simulation verification

The simulation data is generated by Matlab, IMU (inertial measure unit) data with swaying interference. The sloshing interference setting is shown in (28), the interference parameter setting and sensor parameters is shown in table 1 and 2 respectively.

$$\begin{cases} pitch = pitch_m \sin(2\pi k T_s / T_P + pitch_0) + pitch_1 \\ roll = roll_m \sin(2\pi k T_s / T_R + roll_0) + roll_1 \\ yaw = yaw_m \sin(2\pi k T_s / T_Y + yaw_0) + yaw_1 \end{cases} \tag{28}$$

Table 1 The parameters in oscillating base generator

Parameters	Values
Amplitudes	$pitch_m$=5°, $roll_m$=5°, yaw_m=5°
Periods	T_P=14s, T_R=16s, T_Y=18s
Initial phase	$Pitch_0$=5°, $roll_0$=5°, yaw_0=5°
Initial angles	$Pitch_1$=5°, $roll_1$=5°, yaw_1=5°
Discrete time	T_s=0.01s
Simulation time	T=600s

Table 2 The sensor specifications of SINS

Sensors	Constant bias	Random noise
Three-axis gyro	10°/h	1°/h
Three-axis accelerometer	1mg	0.1mg

The simulation results are in Fig. 2.

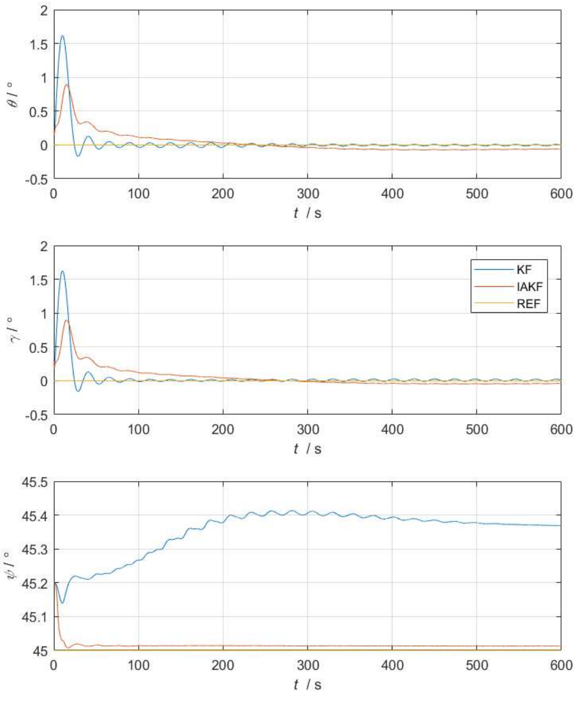

Fig. 2 Comparison chart of fine alignment angle under shaking base.

Fig. 2 is a comparison diagram of the angle alignment results of the classic Kalman filter and IAKF in the paper. The yellow line REF in Fig. 2 represents the true value, and Fig. 3 is the error comparison. It can be seen that the improved algorithm can estimate the attitude angle well, and the convergence accuracy is high after about 100s. The pitch, roll and heading error are basically kept within 10 divisions, while the Kalman filter has a large error in the estimation of the heading, and the result is poor. Moreover, it cannot converge to the true value well, and the work effect is not ideal. The reason is mainly because the Kalman filter has high requirements on the accuracy of model construction, and the sensitivity of noise parameters and system parameters is high so that it is easily affected by these uncertain parameters. IAKF reduces the effect of the Kalman filter. The dependence of these parameters has higher robustness and is more suitable for practical use.

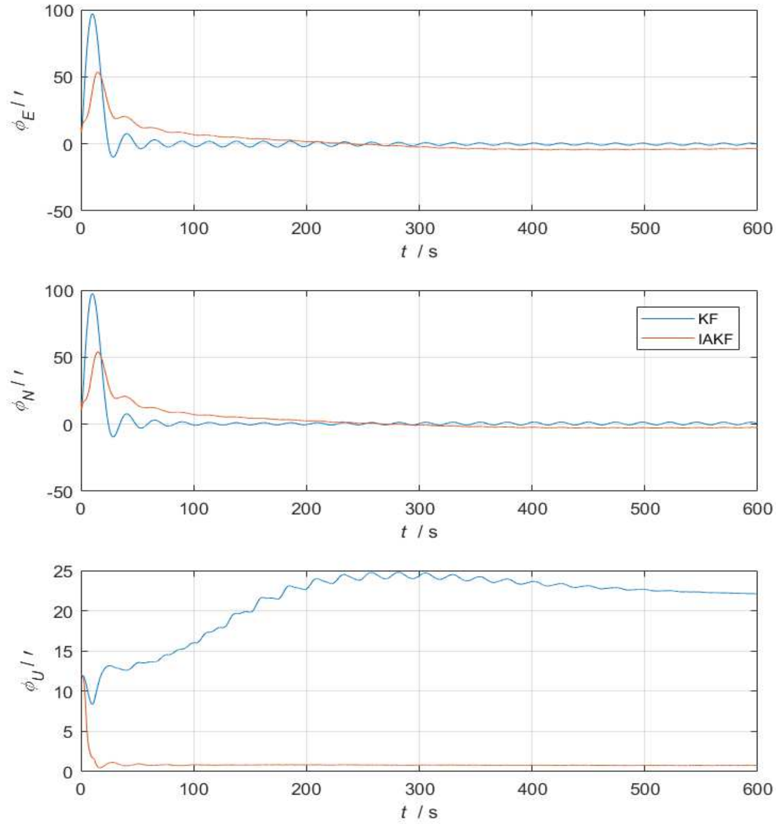

Fig. 3 Comparison chart of precision alignment error under shaking base.

Then, this paper changed the shaking condition settings, increased the oscillation amplitude and period, set the oscillation amplitude to 6 degrees, and the period at 24s. The simulation results are in Fig. 4.

It can be seen from Fig. 4 that after the shaking interference is increased, the Kalman filter leads to a divergence phenomenon, and the alignment result results to a malformed waveform, which can no longer reflect the alignment result. The result is not even as high as the coarse alignment accuracy, and the fine alignment is lost notably.

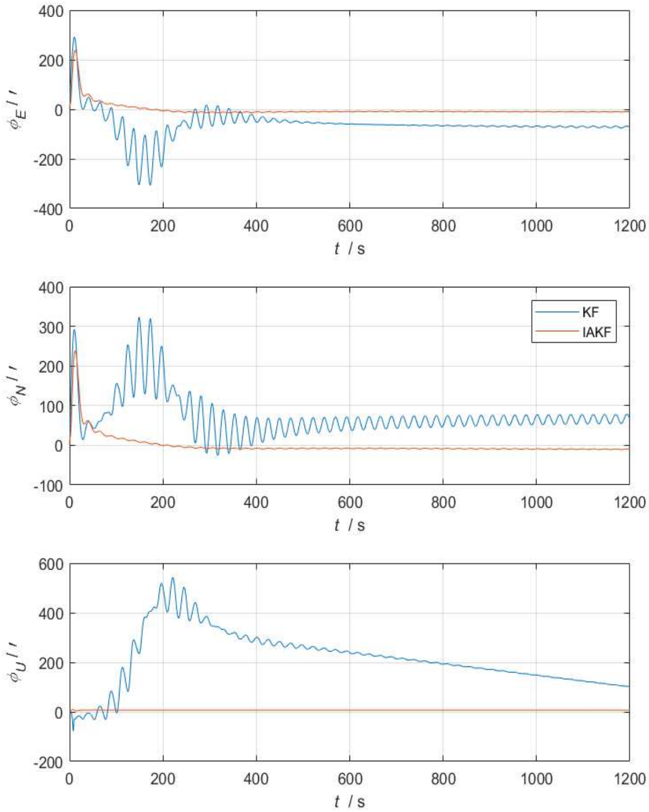

Fig. 4 Comparison of alignment errors with changing shaking conditions.

In order to better illustrate the anti-jamming improvement effect of the proposed method in the paper, the paper changes the oscillation frequency on the basis of the same oscillation amplitude to do 2 sets of comparison simulations. The average value of 200s alignment results under the same conditions is selected as the result of each simulation. The result is shown in table 3 (min represents 1/60 degrees).

Table 3 Comparison table of results of two filtering methods under different oscillation conditions

		Φ_E Mean		Φ_N Mean		Φ_U Mean	
		KF /min	IAKF/min	KF/min	IAKF/min	KF/min	IAKF/min
The amplitude is 3°.	Cycle 14s	10.02	-3.13	-2.56	1.65	-40.96	4.85
	Cycle 24s	50.64	-4.65	-98.65	-5.64	-519.65	2.68
	Cycle 34s	-150.32	-8.76	90.68	-6.78	-915.62	2.46
Oscillation period is 24s.	Amplitude 2°	45.86	-4.89	-70.96	-5.14	-436.52	2.46
	Amplitude 4°	76.58	-12.62	-80.65	-11.34	-550.63	3.56
	Amplitude 6°	-156.53	-15.62	-105.62	-12.65	-736.48	7.64

It can be seen from table 3 that the alignment result of the classic KF changes with the interference, and fluctuates greatly, especially after the interference amplitude becomes larger and the interference frequency decreases. The alignment result has diverged and lost its reference. This is mainly because KF filtering is easily affected by the historical value. As the interference frequency decreases, the historical value changes slowly so that the historical value has a stronger and stronger interference effect on the result, resulting in a large deviation of the result. IAKF alignment results show little fluctuations, and the simulation results are basically stable within 10 min. The improved algorithm has greatly improved the correction of large swings and historical values. The result is obviously better than the classic Kalman filter, and the anti-interference ability is very good.

3.2 Real measurement verification

The paper selects Redmi K30Pro mobile phone as the data acquisition hardware tool, and uses Matlab mobile phone version as the software tool to place the mobile phone horizontally on the horizontal cooling fan, and then adjust the fan's rotation rate as the main source of shaking. The placement method is shown in Fig. 5. From left to right and top to bottom, there are corresponding schematic diagrams of directions 1, 2, 3, and 4 respectively. The base is an adjustable speed fan, and a Redmi phone is on the top of the fan.

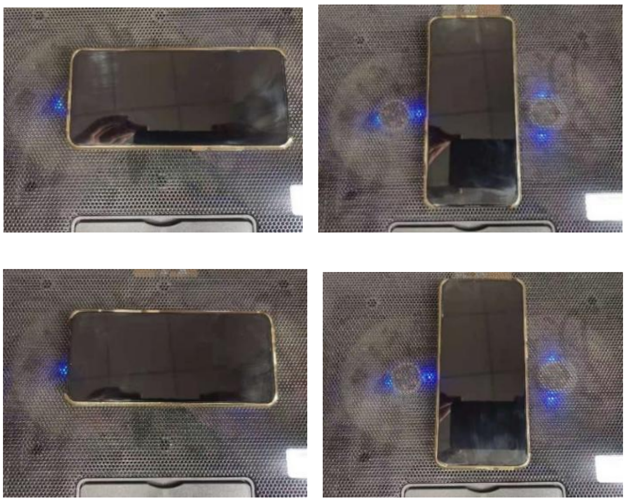

Fig. 5 Placement diagram.

A total of four azimuth data were collected, and five sets of data were collected for each azimuth. We used IAKF in the paper and classic Kalman filter do initial alignment experiments. The coarse alignment stage uses the same method, and the same coarse alignment result is used as the fine alignment input. The results are shown in Fig. 6 ~ 8.

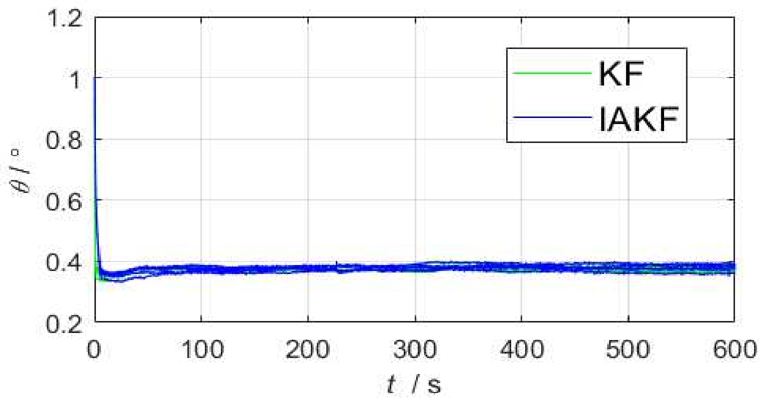

Fig. 6 The result of five-time pitch alignment of azimuth three.

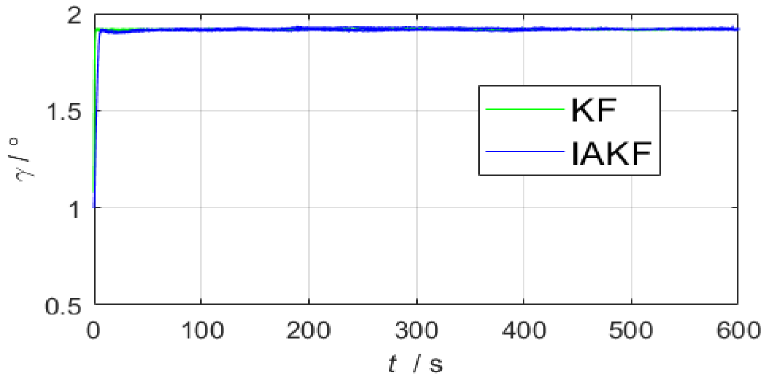

Fig. 7 The result of five-time roll alignment of azimuth three.

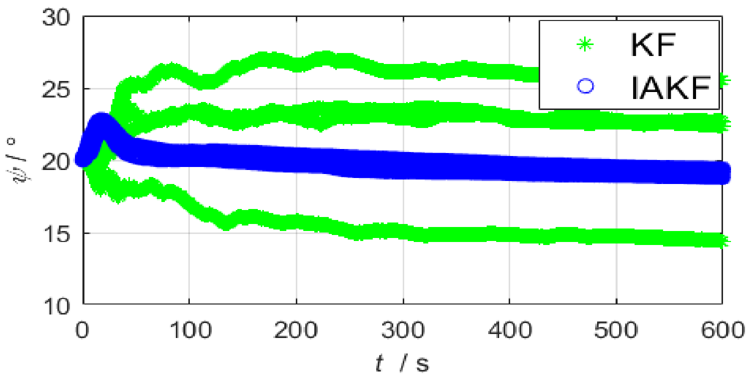

Fig. 8 The result of five-time heading alignment of azimuth one.

The pitch and roll of azimuth 2 to azimuth 4 are basically the same as the waveform of azimuth 1, and the comparison results of the two methods are also basically the same, which the convergence consistency is relatively good. The following mainly lists the heading comparison of the other three azimuths in Fig. 9 ~ 11.

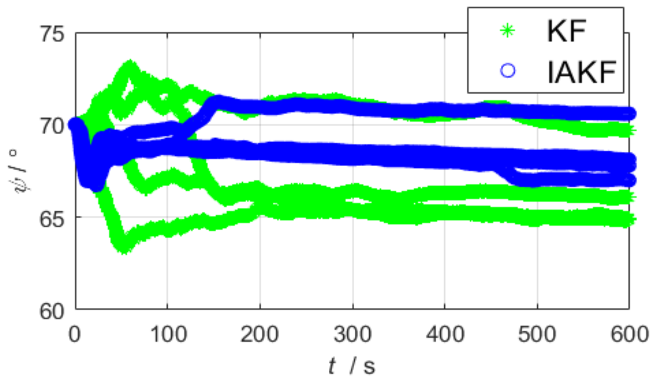

Fig. 9 The result of five-time heading alignment of azimuth two.

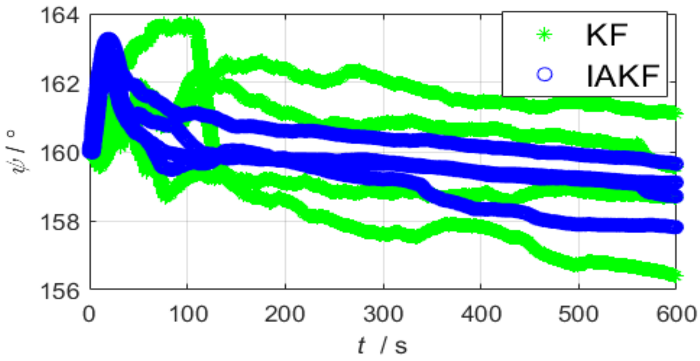

Fig. 10 The result of five-time heading alignment of azimuth three.

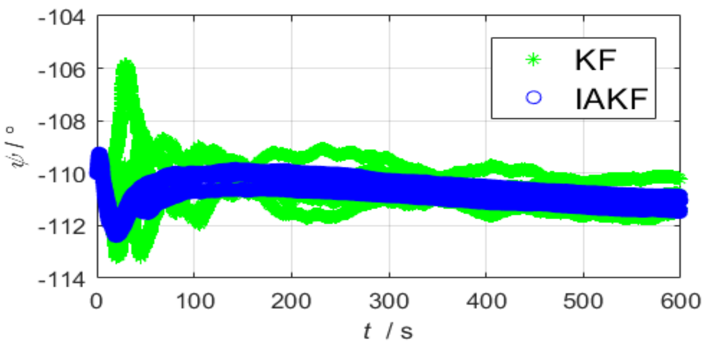

Fig. 11 The result of five-time heading alignment of azimuth four.

In order to further verify the effect of the improved algorithm, Monte Carlo simulation is carried out for the data collected from four directions. Each azimuth data is simulated for 1000 times, and the mean square error is calculated. The test results are shown in Fig. 12 ~ 15.

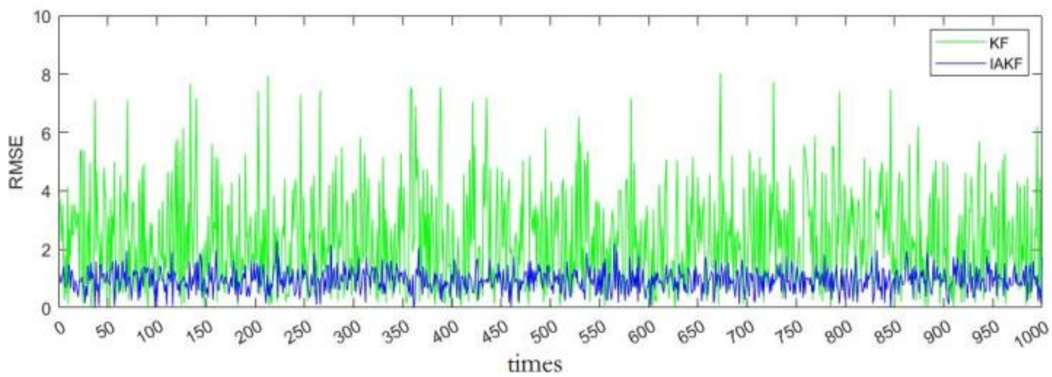

Fig. 12 RMSE result of Monte Carlo simulation of Azimuth one.

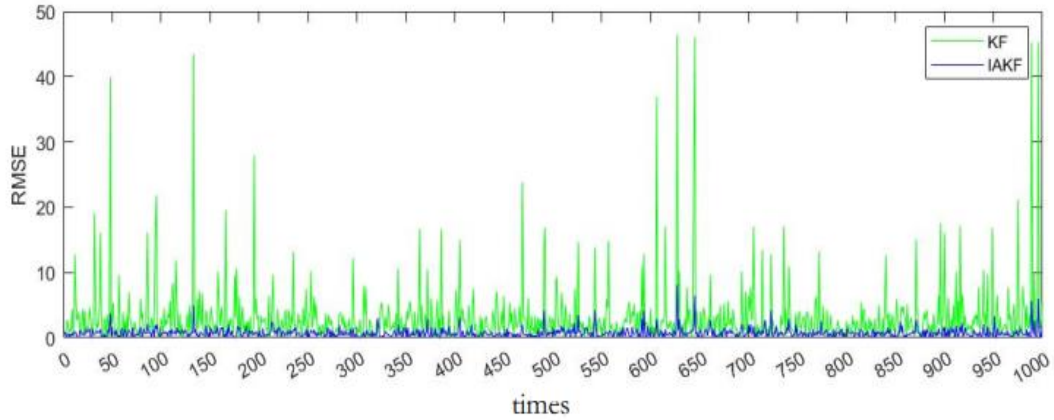

Fig. 13 RMSE result of Monte Carlo simulation of Azimuth two.

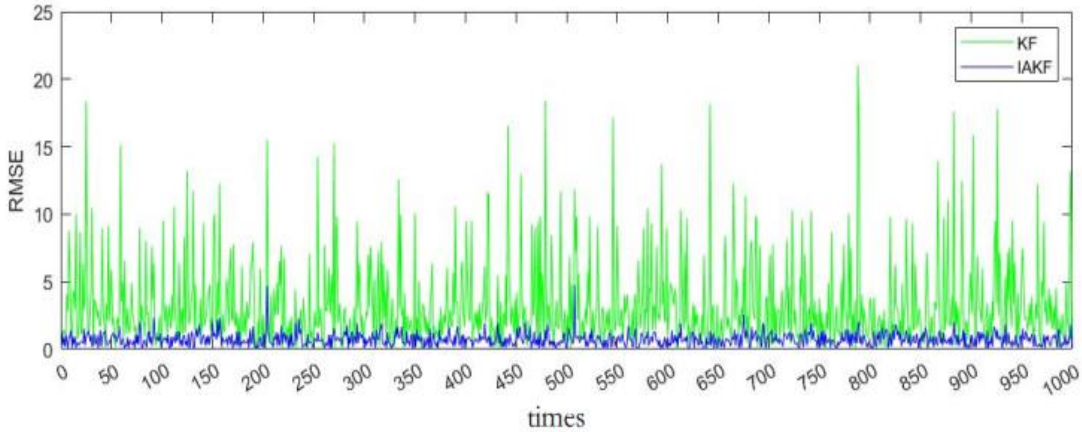

Fig. 14 RMSE result of Monte Carlo simulation of Azimuth three.

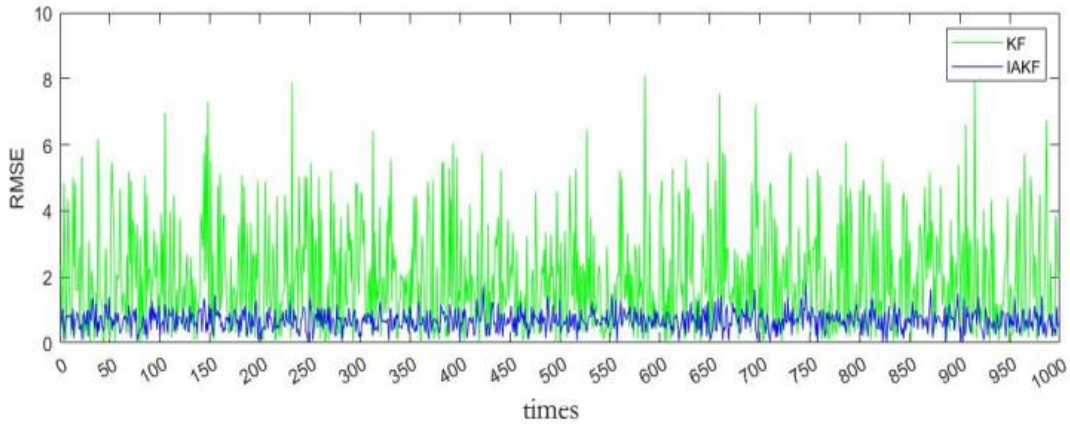

Fig. 15 RMSE result of Monte Carlo simulation of Azimuth four.

The inertial sensor of the mobile phone is a MEMS series sensor with a slightly lower accuracy, and the estimation of the heading has a large deviation and inaccuracy, but it can be used to judge the stability of the algorithm. The two algorithms use the same data, the same precise input, and judge the pros and cons based on the consistency of the final results. It can be seen that the improved algorithm results have higher convergence consistency and relatively stable results, while the traditional Kalman filtering algorithm has poor convergence consistency. Although the final result of each curve has become smooth and stable, there is a difference between the curves. The difference is large, it cannot reflect the alignment result well, and the credibility is low.

The improved algorithm can detect the stability of the filtering, and when the filtering abnormality is detected, the noise parameters in the filtering process can be adjusted to avoid filtering divergence. Moreover, the improved algorithm increases the correction effect of the measurement on the state estimation, and can quickly reduce the influence of the historical value with low credibility, and further increase the reliability of the result.

4. Conclusion

This paper proposes an improved Kalman filter algorithm (IAKF) based on the initial alignment under the shaking base. The traditional Kalman filter is prone to divergence anomalies due to inaccurate modeling. To solve this problem, this paper combines the sequence inertial filtering algorithm to improve the filter noise parameter update process, and adds a filter anomaly detection mechanism based on the detection results. The update mode corresponding to different selections suppresses the filtering divergence to a certain extent and reduces the dependence on the accuracy of the model parameters. In addition, the Kalman filter gain matrix update method was improved by combining the fading factor filtering, which increased the correction effect of the measurement on the state estimation. The results of experiments show that the improved method can approximate the true value faster and reduce the alignment time. The proposed method can be applied in smart phone navigation with the strapdown inertial navigation system, such as vehicle-mounted inertial navigation, unmanned aerial vehicle, person navigation, and so on.

Declarations

This work was partially supported by Shaanxi provincial fund of China (Grant numbers 2020JM-185).

Financial interests: The authors have no relevant financial or non-financial interests to disclose.

Not applicable availability of data and material.

Not applicable code availability.

Not applicable authors' contributions.

References

1. X. Xu, J. Gui, Y. Sun, Y. Yao and T. Zhang. (2021). A robust in-motion alignment method with inertial sensors and Doppler velocity log. *IEEE Trans. Instrum. Meas*, *70,* 1-13.
2. Y. Huang, Z. Zhang, S. Du, Y. Li and Y. Zhang. (2020). A high-accuracy GPS-aided coarse alignment method for MEMS-based SINS. *IEEE Trans. Instrum. Meas*, *69*, 7914-7932
3. J. Xu, H. He, F. Qin and L. Chang. (2017). A novel autonomous initial alignment method for strapdown inertial navigation system. *IEEE Trans. Instrum. Meas, 66*, 2274-2282.
4. T. Zhang, L. Chen and Y. Yan. (2018). Underwater positioning algorithm based on SINS/LBL integrated system. *IEEE Access*, *6,* 7157-7163.
5. T. Jinwu, X. Xiaosu, Z. Tao, Z. Liang and L. Yao. (2018). Study on installation error analysis and calibration of acoustic transceiver array based on SINS/USBL integrated system. *IEEE Access, 6,* 66923-66939.

6. L. Chang, J. Li and S. Chen. (2015). Initial alignment by attitude estimation for strapdown inertial navigation systems. *IEEE Trans. Instrum. Meas, 64,* 784-794.
7. M. Cong, H. Lu, X. Cheng and H. Liang. (2019). Transfer alignment method and realization of SINS on moving base based on Kalman filter. *2019 IEEE 1st International Conference on Civil Aviation Safety and Information Technology*, 329-333.
8. X. Cui, G. Yan, Q. Fu, Q. Zhou and Z. Liu. (2018). A unified nonsingular rapid transfer alignment solution for tactical weapon based on matrix Kalman filter. *IEEE Access, 6,* 78700-78709.
9. G. Zhang, C. Lu and Y. Li. (2019). Research on initial alignment method of SINS with improved CKF. *IEEE 3rd Information Technology, Networking, Electronic and Automation Control Conference,* 2315-2319.
10. F. Jiancheng and Y. Sheng. (2011). Study on innovation adaptive EKF for in-flight alignment of airborne POS. *IEEE Trans. Instrum. Meas, 60,* 1378-1388.
11. G. Xu, Y. Huang, Z. Gao and Y. Zhang. (2020). A computationally efficient variational adaptive Kalman filter for transfer alignment. *IEEE Sensors Journal, 20,* 13682-13693
12. B. Wang, W. Ye and Y. Liu. (2020). An improved real-time transfer alignment algorithm based on adaptive noise estimation for distributed POS. *IEEE Access, 8,* 102119-102127.
13. D. Huang, H. Leung and N. EL-Sheimy. (2007). Expectation maximization based GPS/INS integration for land-vehicle navigation. *IEEE Trans. Aerospace and Electronic Systems, 43,* 1168-1177.
14. Y. Huang, Y. Zhang, B. Xu, Z. Wu and J. A. Chambers. (2018). A new adaptive extended Kalman filter for cooperative localization. *IEEE Trans. Aerospace and Electronic Systems, 54,* 353-368.
15. S. Julier, J. Uhlmann and H. F. Durrant-Whyte. (2000). A new method for the nonlinear transformation of means and covariances in filters and estimators. *IEEE Trans. Automatic Control, 45,* 477-482.
16. F. Pei, S. Yang and S. Yin. (2021). In-motion initial alignment using state-dependent extended Kalman filter for strapdown inertial navigation system. *IEEE Trans. Instrum. Meas, 70,* 1-12.
17. S. Guo, J. Xu and Z. Cheng. (2017). Inertial navigation system alignment based on fading Kalman filter and fixed point smoother. *10th International Symposium on Computational Intelligence and Design,* 279-282.
18. G. Yan, X. Yang, X. Su, J. Weng and Y. Qin. (2018). Error distribution method and analysis of observability degree based on the covariances in Kalman filter. *37th Chinese Control Conference,* 4900-4905.

Supplementary Files

This is a list of supplementary files associated with this preprint. Click to download.

- AuthorsPictureBiography.doc